

Fabrication of dense β -calcium orthophosphate with submicrometer-sized grains and its high-temperature superplastic deformation

Daisuke Watanabe · Keishi Nishio · Yoshio Sakka · Masataka Ohgaki · Ian J. Davies · Tomohiro Umeda · Seiichiro Koda · Kiyoshi Itatani

Received: 7 July 2010 / Accepted: 25 October 2010 / Published online: 12 November 2010
© Springer Science+Business Media, LLC 2010

Abstract High-density β -calcium orthophosphate (β -Ca₃(PO₄)₂, also called β -tricalcium phosphate: β -TCP) ceramics with submicrometer-sized grains were fabricated using a pulse-current pressure firing route. The maximum relative density of the β -TCP compacts was 98.7% at 1050 °C and this was accompanied by a translucent appearance. The mean grain size of the β -TCP compacts increased slightly with temperature to reach 0.78 μ m at 1000 °C. However, upon further increasing the firing temperature to 1050 °C the mean grain size increased significantly to 1.6 μ m. The extent of plastic deformation during tensile testing was examined at temperatures between 900 and 1100 °C using a strain rate in the range 9.26×10^{-5} to 4.44×10^{-4} s⁻¹. The maximum tensile

strain achieved was 145% for a test temperature of 1000 °C and strain rate of 1.48×10^{-4} s⁻¹ and this was attributed to the relatively high density and small grain size.

Introduction

While ceramics possessing ionic and covalent bonding are generally mechanically hard, heat-resistant, and wear-resistant, they are also brittle, giving rise to potential difficulties during fabrication of components into complex shapes. With a view to overcoming these potential difficulties, injection molding and other techniques have been utilized to fabricate complex-shaped ceramic materials. In addition to these techniques, the potential exists for significant plastic deformation or superplasticity of polycrystalline ceramic materials with submicrometer-sized grains at elevated temperature [1]. Typical examples of superplastic behavior include Al₂O₃-dispersed tetragonal zirconia (ZrO₂) (tensile strain: 1000%) [2] and 40ZrO₂(3Y)–30MgAl₂O₄–Al₂O₃ (tensile strain: 2500%) [3] with the phenomenon of superplasticity being a key factor for the fabrication of intricately shaped ceramics.

The superplasticity of hydroxyapatite (Ca₁₀(PO₄)₆(OH)₂; HAp) has previously been examined by Wakai et al. [4], who reported that the tensile strain of HAp specimens fabricated by hot isostatic pressing attained 153%. More recently, the present authors have also investigated the densification behavior and high-temperature superplastic deformation of pressurelessly fired HAp specimens with a relative density of 99.2% and mean grain size of 0.56 μ m; the tensile elongation at 1100 °C was found to be 157% [5]. Furthermore, use of a two-step firing technique reduced the mean grain size to 0.44 μ m in combination with a relative density of 98.8%. Following adoption of this two-step firing procedure, the

D. Watanabe · T. Umeda · S. Koda · K. Itatani (✉)
Department of Materials and Life Sciences, Faculty of Science and Engineering, Sophia University, 7-1 Kioi-cho, Chiyoda-ku, Tokyo 102-8554, Japan
e-mail: itatani@sophia.ac.jp

K. Nishio
Department of Materials Science and Technology, Faculty of Industrial Science and Technology, Tokyo University of Science, 2641 Yamazaki, Noda, Chiba 278-8510, Japan

Y. Sakka
International Center for Materials Nanoarchitectonics and Nano Ceramics Center, National Institute for Materials Science, 2-1, Sengen1-chome, Tsukuba-shi, Ibaraki 305-0047, Japan

M. Ohgaki
Beam Technology Application Engineering Department, SII NanoTechnology Inc., 1-18-2, Hakusan, Midori-ku, Yokohama-shi, Kanagawa 226-0006, Japan

I. J. Davies
Department of Mechanical Engineering, Curtin University, GPO Box U1987, Perth, WA 6845, Australia

tensile elongation was further improved to 188% [6]. Finally, HAp specimens with a relative density of 99.7% and grain size as low as 0.21 μm have been fabricated utilizing a pulse-current pressure firing technique; the maximum tensile strain of these HAp specimens achieved 286% [7]. These results would appear to confirm that submicrometer-sized grains are required for the superplastic deformation of HAp ceramics.

As a next step, the authors' attention has been directed toward the high-temperature superplastic deformation of β -calcium orthophosphate ($\beta\text{-Ca}_3(\text{PO}_4)_2$, also called β -tricalcium phosphate; β -TCP) specimens with submicrometer-sized grains due to their potential for use in bone-substitution applications [8, 9]. Previously, Kondoh et al. [10] reported that almost fully dense and transparent β -TCP ceramic material with grain sizes below 2 μm could be fabricated using hot isostatic pressing. On the other hand, Kawagoe et al. [11] indicated that transparent β -TCP ceramic material with a relative density of greater than 99% and mean grain size of 1.5 μm could be fabricated using the pulse-current pressure firing technique. However, to the knowledge of the authors, no information concerning the high-temperature superplastic deformation of β -TCP ceramic and its relationship to densification and microstructural development has been available until the present time. In addition, the accumulation of tensile strain data may be helpful for the realization of superplastic deformation techniques to fabricate complex-shaped β -TCP ceramic components.

On the basis of the above information, this article describes (i) the densification behavior of β -TCP ceramic material using pulse-current pressure firing, and (ii) the high-temperature superplastic deformation of resulting β -TCP specimens.

Experimental procedure

Fabrication of dense β -TCP ceramic material with submicrometer-sized grains

A commercially available β -TCP powder was used in this study (β -TCP-100; Taihei-Kagaku Sangyo, Osaka). The primary particle size of the powder measured using the BET technique was 0.108 μm , whereas the secondary particle size was found to be within the range 0.8–4 μm (mean value: 1.28 μm) using a dynamic light-scattering particle size analyzer. Cylindrical compacts with a diameter of 30 mm and thickness of 3 mm were fabricated by uniaxially pressing approximately 12 g of β -TCP powder at 50 MPa and followed by pulse-current pressure firing (pressure: 50 MPa) at a temperature between 900 and 1100 $^\circ\text{C}$ for 5 min with the heating rate being

100 $^\circ\text{C min}^{-1}$. Specimens for tensile testing were prepared with a gauge length of 9 mm from the sintered compacts.

Evaluation

Phase identification was conducted using an X-ray diffractometer (XRD; RINT 2000V/P, Rigaku, Tokyo, Japan, 40 kV and 40 mA) with monochromatic $\text{CuK}\alpha$ radiation. Also, Fourier transform infrared spectrometry (FT-IR; Model 8600PC, Shimadzu, Kyoto, Japan) using the KBr pellet method was carried out to determine functional groups.

The relative density of the sintered compact was calculated on the basis of bulk density and theoretical density ($=3.07 \text{ g cm}^{-3}$); the bulk density was measured using the Archimedes method and ethanol as a replacement liquid. The microstructure of the sintered compact was observed using a scanning electron microscope (SEM; Model S-4500, Hitachi, Tokyo, Japan) with an accelerating voltage of 5 kV. On the basis of SEM micrographs, the distribution of grain sizes was determined as $\pi/2$ times the linear intercept length with a minimum of 300 grains being used for each specimen.

Tensile tests were conducted in air at temperatures between 900 and 1100 $^\circ\text{C}$ using a strain rate between 9.26×10^{-5} and $4.44 \times 10^{-4} \text{ s}^{-1}$ on a universal testing machine (TENSILON-1310, A & D Company, Tokyo, Japan) equipped with an infrared furnace with a minimum of two specimens being used for each testing condition. True stress–strain curves were calculated on the basis that uniform linear deformation occurred during elongation; the true stress was calculated from the initial cross section and resulting strain. The microstructure of a typical deformed specimen was observed using a transmission electron microscope (TEM; Model JEM-2011, JEOL, Tokyo, Japan; accelerating voltage, 200 kV); the specimen was thinned initially by mechanical polishing and then using a focused Ga^+ -ion beam (FIB; Model SMI3050, SII NanoTechnology Inc., Tokyo).

Results and discussion

Pulse-current pressure firing of β -TCP compacts

As the properties of the starting powder are known to influence the sinterability of β -TCP, the presence of crystalline phase(s) and type of particle morphology were first investigated with XRD analysis indicating the only phase present within the starting powder to be β -TCP, while the crystallite size estimated from the β -TCP(2020) peak and Scherrer's formula was found to be 0.108 μm and thus

consistent with the primary particle size obtained using the BET method.

The presence of other phosphate ions, in particular $P_2O_7^{4-}$, was checked using FT-IR. The spectrum of the starting powder contained absorption peaks at 1121, 1043, 970, 943, 606, and 552 cm^{-1} . The absorption peaks at 552 and 606 cm^{-1} were assigned to the O–P–O bending mode within the PO_4^{3-} group, while the peaks at 970 and 1043 cm^{-1} were assigned to the symmetric P–O stretching mode within the PO_4^{3-} group. It was therefore concluded that these absorption peaks were consistent with that of β -TCP with no other phosphate ions (such as $P_2O_7^{4-}$) being present within the powder due to the lack of the characteristic $P_2O_7^{4-}$ peak at 730 cm^{-1} [12].

As mentioned earlier, an important requirement for the superplastic deformation of β -TCP is the need for grain sizes below $1\text{ }\mu\text{m}$. This factor is consistent with the knowledge that superplastic deformation in ceramic materials is associated with grain-boundary sliding that may be promoted with decreasing grain size. In comparison to pressureless firing, which is a standard ceramic processing technique, pulse-current pressure firing is a novel technique that near-instantaneously produces a high-temperature field due to pulse energy, shock pressure by electric discharge and Joule heating. Dense ceramic materials with submicrometer-sized grains have previously been fabricated using this method and, as such, the fabrication conditions of dense β -TCP ceramic material, in addition to the control of grain size, were investigated using this technique.

Changes in the volume shrinkage of a β -TCP compact with increasing temperature due to the application of pulse-current pressure firing have been shown in Fig. 1. The volume shrinkage of the β -TCP compact was noted to start at approximately $800\text{ }^\circ\text{C}$ and increased with temperature up to $1050\text{ }^\circ\text{C}$. On the basis of this information, the

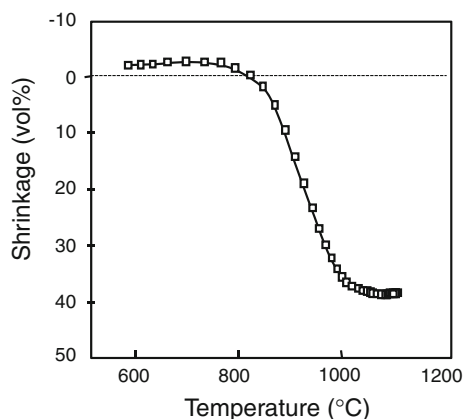


Fig. 1 Effect of temperature on volume shrinkage during pulse-current pressure firing of a β -TCP compact (applied pressure: 50 MPa) under reduced pressure

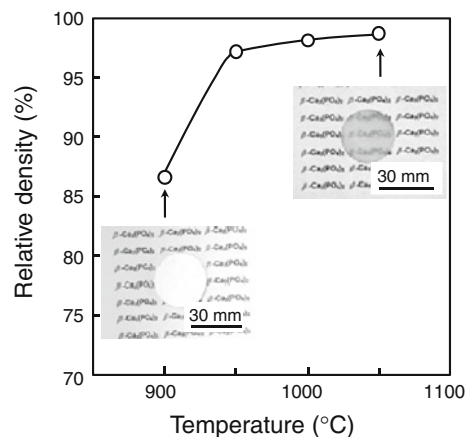


Fig. 2 Effect of firing temperature on the relative density of β -TCP compacts fabricated by pulse-current pressure firing (applied pressure: 50 MPa) for 5 min under reduced pressure, together with typical photographs of the sintered compacts

fabrication conditions of dense β -TCP ceramic material with submicrometer-sized grains were investigated by pulse-current pressure firing above $900\text{ }^\circ\text{C}$ with the influence of firing temperature on relative density having been presented in Fig. 2, together with typical photographs of the sintered β -TCP compact. The relative density of the β -TCP compact was observed to exceed 95% for a firing temperature of $950\text{ }^\circ\text{C}$ and increased to reach a maximum of 98.7% at $1050\text{ }^\circ\text{C}$; the β -TCP compact for this latter case was found to be translucent as shown by the photograph.

The influence of firing temperature on the grain size has been presented in Fig. 3, together with typical FE-SEM micrographs of the sintered β -TCP compacts. The mean grain size of the β -TCP compact fired at $900\text{ }^\circ\text{C}$ was approximately $0.34\text{ }\mu\text{m}$ and this increased slightly with

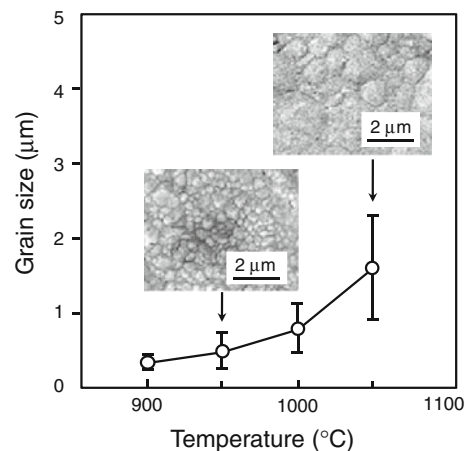


Fig. 3 Effect of firing temperature on the mean grain size of β -TCP compacts fabricated by pulse-current pressure firing (applied pressure: 50 MPa) for 5 min under reduced pressure, together with typical SEM micrographs of the sintered compacts

temperature to reach $0.78\ \mu\text{m}$ at $1000\ ^\circ\text{C}$. However, further increasing the firing temperature to $1050\ ^\circ\text{C}$ significantly increased the mean grain size to $1.6\ \mu\text{m}$. From the results shown in Figs. 2 and 3, it was concluded that dense β -TCP ceramics with submicrometer-sized grains (i.e., the conditions necessary for superplastic deformation) could be fabricated using pulse-current pressure firing at $1000\ ^\circ\text{C}$ for 5 min.

Tensile elongation of β -TCP specimens at high temperature

Tensile tests were carried out for dense β -TCP specimens fabricated using the optimized conditions mentioned in the previous section. First, the influence of test temperature on the tensile behavior of β -TCP specimens was examined with the results being presented in Fig. 4, together with a typical photograph. Note that the firing and tensile test temperatures were set to be the same and thus the porosity and mean grain size were different for each test temperature—the overall strain rate was considered to depend mainly on these three factors, i.e., temperature, porosity, and mean grain size. In each case the true stress initially increased linearly with strain (i.e., elastic deformation) and then, upon reaching a maximum value, gradually decreased with further increases in strain until catastrophic fracture occurred. A maximum tensile strain of 145% was achieved at $1000\ ^\circ\text{C}$ (see photographs in Fig. 4 indicating the original and elongated β -TCP specimens); the tensile strain of each β -TCP specimen was ordered with respect to test temperature as follows: 145% at $1000\ ^\circ\text{C}$ > 143% at $950\ ^\circ\text{C}$ > 70.2% at $1050\ ^\circ\text{C}$ > 58.7% at $900\ ^\circ\text{C}$.

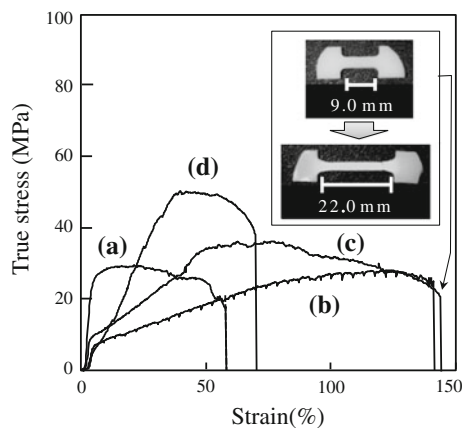


Fig. 4 True stress–strain curves of β -TCP specimens at test temperatures of (a) $900\ ^\circ\text{C}$, (b) $950\ ^\circ\text{C}$, (c) $1000\ ^\circ\text{C}$, and (d) $1050\ ^\circ\text{C}$ (strain rate: $1.48 \times 10^{-4}\ \text{s}^{-1}$), together with the photographs of as-fabricated (above) and tested (below) specimens. Note that each β -TCP specimen was manufactured from a cylindrical specimen fabricated using pulse-current pressure firing (applied pressure: 50 MPa) for 5 min under reduced pressure, and that the test temperature was the same as the firing temperature

The above results indicate that a maximum tensile strain of 145% could be achieved when the β -TCP specimen was fabricated using pulse-current pressure firing at $1000\ ^\circ\text{C}$ for 5 min. Since the relative density and grain size of the β -TCP specimen fired at $1000\ ^\circ\text{C}$ for 5 min were 98.1% and $0.78\ \mu\text{m}$, respectively (see Figs. 2, 3), the presence of a smaller mean grain size, when compared to the specimen fired at $1050\ ^\circ\text{C}$ for 5 min, was believed to have promoted grain-boundary sliding [13] and thus resulted in superior superplastic performance. A similar effect was also evident for the specimen fired at $950\ ^\circ\text{C}$ which also possessed a small mean grain size and high relative density.

The influence of strain rate on the true stress–strain behavior of β -TCP specimens fired at $1000\ ^\circ\text{C}$ has been presented in Fig. 5. Similar to the effect of temperature mentioned above, the overall trend showed the true stress to initially increase with strain prior to reaching a maximum value and followed by a slowly decreasing stress until catastrophic failure occurred. The tensile strain was the largest for a strain rate of $1.48 \times 10^{-4}\ \text{s}^{-1}$ and decreased as the strain rate increased further to $4.44 \times 10^{-4}\ \text{s}^{-1}$; the maximum tensile strain was ordered as follows: 145% at $1.48 \times 10^{-4}\ \text{s}^{-1}$ > 136% at $2.96 \times 10^{-4}\ \text{s}^{-1}$ > 93.4% at $9.26 \times 10^{-5}\ \text{s}^{-1}$ > 72.6% at $4.44 \times 10^{-4}\ \text{s}^{-1}$.

These results indicate that an optimum strain rate, i.e., $1.48 \times 10^{-4}\ \text{s}^{-1}$, exists with regards to maximum tensile strain and hence superplastic behavior. When the strain rate was low, e.g., $9.26 \times 10^{-5}\ \text{s}^{-1}$, premature failure was concluded to have occurred due to the presence of intergranular cavitation and grain growth [14] as a result of the increased heating time. In contrast to this, the suppression of grain-boundary sliding, attributed to dislocation and grain switching with neighboring grains (to maintain an

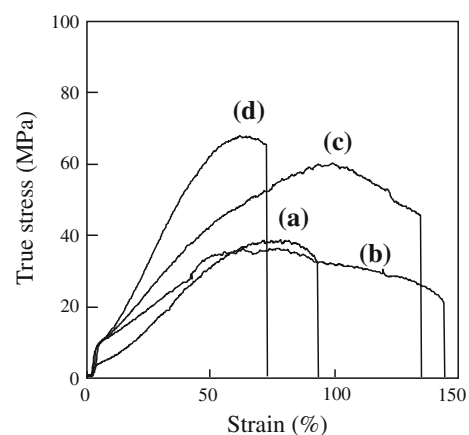


Fig. 5 True stress–strain curves of β -TCP specimens at $1000\ ^\circ\text{C}$ under strain rates of (a) $9.26 \times 10^{-5}\ \text{s}^{-1}$, (b) $1.48 \times 10^{-4}\ \text{s}^{-1}$, (c) $2.96 \times 10^{-4}\ \text{s}^{-1}$, and (d) $4.44 \times 10^{-4}\ \text{s}^{-1}$ in air. Note that each β -TCP specimen was manufactured from a cylindrical specimen fabricated using pulse-current pressure firing (applied pressure: 50 MPa) at $1000\ ^\circ\text{C}$ for 5 min under reduced pressure

equiaxed shape), was thought to have contributed to premature failure at high strain rates, i.e., greater than $1.48 \times 10^{-4} \text{ s}^{-1}$ [15].

The relationship between strain rate ($\dot{\epsilon}$) and true stress (σ_0) can be expressed as follows: [16]

$$\dot{\epsilon} = \left(\frac{A\sigma_0^n}{d^p} \right) \exp\left(-\frac{Q}{RT}\right) \quad (1)$$

where n is the stress exponent, d is the grain size, p is the grain size exponent, Q is the activation energy, R is the gas constant, T is the temperature, and A is a constant. While it is clear from Fig. 5 that a steady state flow stress is not attained for the testing conditions employed, from consideration that the maximum true stress, σ_0^{max} , represented a consistent superplastic stress feature within each true stress–strain curve (i.e., the maximum superplastic stress that could be sustained at any given strain rate), a semi-quantitative estimation of n was obtained from plotting σ_0^{max} versus $\dot{\epsilon}$ with the results being presented in Fig. 6. The stress exponent for the β -TCP specimens under consideration was found to be approximately 1.9 and similar to that reported by Wakai et al. [17] for yttria-stabilized ZrO_2 specimens. Taking into consideration that the present stress component was below 3, the true stress–strain behavior for the present β -TCP specimens was considered to be a superplastic phenomenon [18].

SEM micrographs and surface grain-size distributions for β -TCP specimens before and after tensile testing at 1000 °C have been presented in Fig. 7. The SEM micrograph and grain-size distribution for the as-fabricated β -TCP specimen indicated the mean grain size to be 0.78 μm with no distinct pores being noted (Fig. 7a, a'). In contrast to this, the deformed β -TCP specimen was

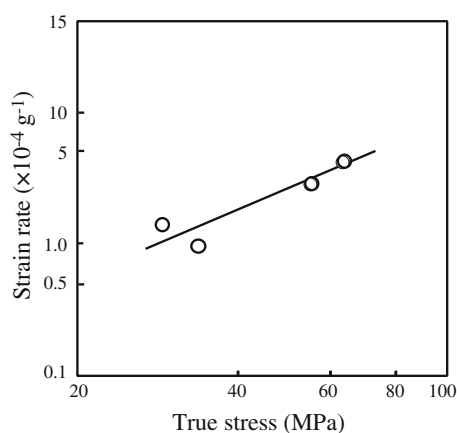


Fig. 6 Maximum true stress versus strain rate for β -TCP specimens at 1000 °C with the gradient of the line (approximately 1.9) being equal to the stress exponent in Eq. 1. Note that each β -TCP specimen was manufactured from a cylindrical specimen fabricated using pulse-current pressure firing (applied pressure: 50 MPa) at 1000 °C for 5 min under reduced pressure

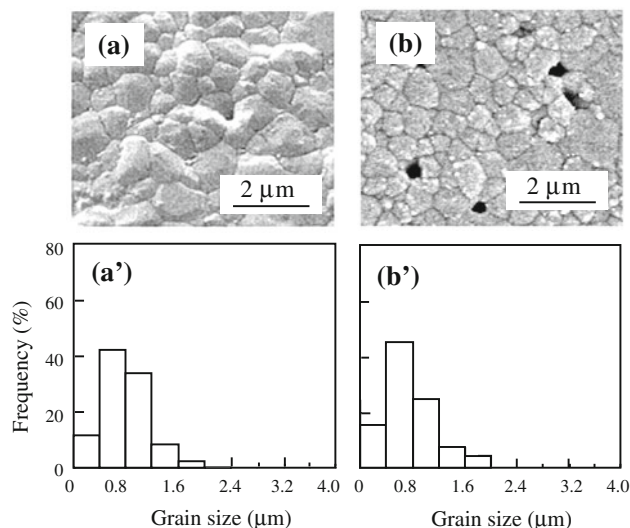


Fig. 7 SEM micrographs and grain-size distributions of β -TCP specimens fabricated by pulse-current pressure firing at 1000 °C for 5 min (applied pressure: 50 MPa) under reduced pressure. (a), (a') As-fabricated β -TCP specimen (b), (b') β -TCP specimen following tensile testing (strain rate: $1.48 \times 10^{-4} \text{ s}^{-1}$) at 1000 °C

composed of closely packed grains with a mean grain size of 0.80 μm with the presence of cavities being noted on grain boundaries (Fig. 7b, b').

No significant change in grain size was noted following the tensile test, giving credence to the suggestion that grain-boundary sliding and grain switching may have occurred in preference to diffusion through the grain boundaries. Furthermore, the creep cavities noted in Fig. 7b appeared to be relatively small, contrary to what had been expected prior to the test. Therefore, further improvements in tensile strain may be anticipated for a reduction of defect density within the β -TCP ceramic below its current value.

The presence of crystalline phases following deformation of the specimen pulse-current pressure fired at 1000 °C for 5 min was checked. Typical XRD patterns for the β -TCP specimens before and after tensile testing have been presented in Fig. 8. While the only phase detected in specimens before and after tensile testing was β -TCP, the relative intensity of the (110), (220), and (214) reflections compared to the (0210) reflection before (Fig. 8a) and after (Fig. 8b) tensile testing suggested the existence of preferred orientation in these β -TCP ceramics and presumed to have taken place during superplastic deformation.

A dark-field TEM micrograph of the same β -TCP specimen (i.e., following tensile testing) has been shown in Fig. 9. Numerous white lines, corresponding to straining of the crystal lattice and/or the presence of dislocations, were observed within the β -TCP matrix. These white lines were sometimes aligned parallel to one another and in other cases aligned randomly. These results strongly suggest that

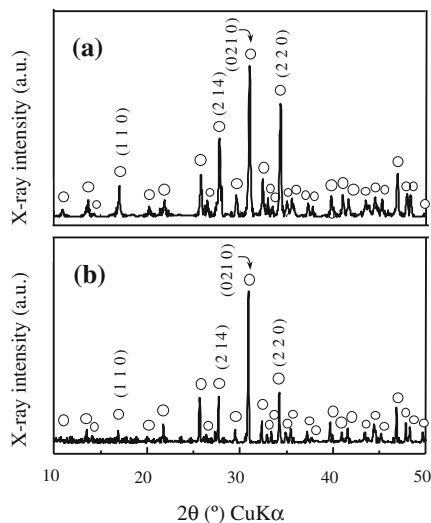


Fig. 8 XRD patterns of β -TCP specimens fabricated by pulse-current pressure firing at 1000 °C for 5 min (applied pressure: 50 MPa) under reduced pressure. **(a)** As-fabricated β -TCP specimen, **(b)** β -TCP specimen following tensile testing (strain rate: $1.48 \times 10^{-4} \text{ s}^{-1}$) at 1000 °C. *Open circle* β -TCP

deformation of the β -TCP specimen may also have been influenced by the presence of densely aligned dislocations and/or sub-boundaries within the β -TCP grains. However, the authors considered that enhanced diffusion at the grain boundaries was the main plastic deformation mechanism. The introduction of lattice strains and/or dislocations may have also contributed to X-ray diffraction results showing the (110), (220), and (214) reflections to have been preferentially reduced following tensile testing.

Overall, it was considered that the lack of any appreciable change in grain size and number of cavities (Fig. 7) was consistent with grain rearrangement due to enhanced diffusion

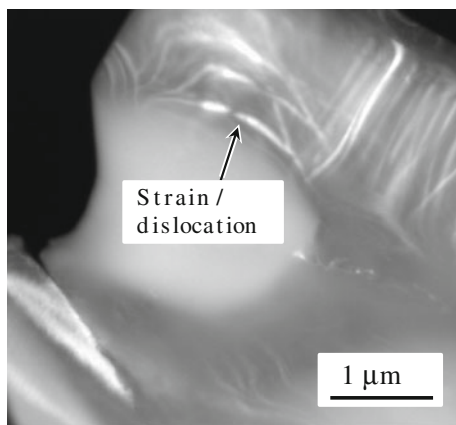


Fig. 9 Typical dark-field TEM micrograph of a β -TCP specimen following tensile testing at 1000 °C. Note that the β -TCP specimen was manufactured from a cylindrical specimen fabricated using pulse-current pressure firing (applied pressure: 50 MPa) at 1000 °C for 5 min under reduced pressure

at the grain boundary being the main mechanism for plastic deformation. While the presence of dislocations was noted in Fig. 9, this was considered to have only a secondary or minor role for plastic deformation within the specimens.

Conclusions

The high-temperature superplastic deformation behavior of dense β -TCP specimens with submicrometer-sized grains fabricated using pulse-current pressure firing was examined. The results obtained were summarized as follows:

- (i). The relative density increased to 98%, while the mean grain size was below 1 μm (i.e., 0.78 μm), for the case of the β -TCP ceramic fabricated using pulse-current pressure firing at 1000 °C for 5 min.
- (ii). The high-temperature superplastic deformation of β -TCP specimens was measured at a temperature between 900 and 1100 °C and at a strain rate between 9.26×10^{-5} and $4.44 \times 10^{-4} \text{ s}^{-1}$. The maximum tensile strain achieved 145% for the test temperature of 1000 °C and a strain rate of $1.48 \times 10^{-4} \text{ s}^{-1}$. While enhanced diffusion at the grain boundaries was considered to be the main mechanism for plastic deformation within these specimens, TEM analysis of the deformed β -TCP specimen also noted the presence of extensive lattice strains and/or dislocations.

Acknowledgments The authors would like to thank Ms. S. Yanagisawa, SII Nanotechnology, Inc., for her assistance with preparing the TEM sample.

References

1. Langdon TG (2009) J Mater Sci 44:5998. doi:10.1007/s10853-009-3780-5
2. Sakka Y, Suzuki TS, Morita K, Nakano K, Hiraga K (2001) Scripta Mater 44:2075
3. Hiraga K, Kim BN, Morita K, Suzuki TS, Sakka Y (2005) J Ceram Soc Jpn 113:191
4. Wakai F, Kodama Y, Sakaguchi S, Nonami T (1990) J Am Ceram Soc 73:457
5. Tago K, Itatani K, Suzuki TS, Sakka Y, Koda S (2005) J Ceram Soc Jpn 113:669
6. Itatani K, Kobayashi A, Watanabe D, Davies IJ, Koda S (2009) J Inorg Mater Japan 16:8
7. Watanabe D, Tago K, Davies IJ, Sakka Y, Itatani K (2009) Phosphorus Lett 66:14
8. Dorozhkin SV (2008) J Mater Sci 43:3028. doi:10.1007/s10853-008-2527-z
9. Dorozhkin SV (2009) J Mater Sci 44:2343. doi:10.1007/s10853-008-3124-x
10. Kondoh I, Tamari N, Kinoshita M (1989) J Ceram Soc Jpn 97:965

11. Kawagoe D, Ioku K, Fujimori H, Goto S (2004) *J Ceram Soc Jpn* 112:462
12. Salah E, Heinrich JG (2003) *Br Ceram Trans* 102:79
13. Padmanabhan KA (2009) *J Mater Sci* 44:2226. doi:[10.1007/s10853-008-3076-1](https://doi.org/10.1007/s10853-008-3076-1)
14. Yang D, Conrad H (2008) *J Mater Sci* 43:4475. doi:[10.1007/s10853-008-2653-7](https://doi.org/10.1007/s10853-008-2653-7)
15. Ashby MF, Verrall RA (1973) *Acta Metall* 2:149
16. Zhan GD, Mitomo M, Nishimura TK, Xie RJ, Sakuma T, Ikuhara Y (2000) *J Am Ceram Soc* 83:841
17. Wakai F, Sakaguchi S, Matsuno Y (1986) *Adv Ceram Mater* 1:259
18. Cannon WR, Langdon TG (1988) *J Mater Sci* 23:1. doi:[10.1007/BF01174028](https://doi.org/10.1007/BF01174028)